Statistics of Radar Backscatter from Wind Waves

David G. Long, Ryan Reed, David V. Arnold

Electrical and Computer Engineering Department, Brigham Young University
459 CB, Provo, UT 84602
(801) 378-4383 fax: (801) 378-6586 long@ee.byu.edu

Abstract - **Measurements of wind wave scattering made by the Yscat ultra wide-band radar are used to study the statistics of the sea surface radar backscatter. As a comparison tool, a simple model based on composite Bragg scattering theory is developed and incorporated in a Monte Carlo simulation. The power and velocity distributions are computed from both empirical and simulated data. Comparison suggests that the composite scattering model accurately predicts the qualitative behavior of the radar return for incidence angles between 30° and 50° for both V and H polarization, but that other scattering mechanisms begin to influence the return at 20° and 60° incidence angles. While it has been postulated that additional scattering mechanisms (e.g., wave breaking and wedge scattering) may contribute to the total scattering, our results suggest that such scatterers do not significantly contribute to the total radar cross section for incidence angles between 30° and 50°.**

I. INTRODUCTION

The Yscat scatterometer was deployed for six months in 1994 on the Canada Center for Inland Waters (CCIW) Research Tower at Lake Ontario and collected over 3500 hours of data at 2-18 GHz and a variety of wind speeds, relative azimuth angles, and incidence angles. This paper considers the distribution of the radar cross section and the velocity in terms of the composite model. Section II describes the Yscat94 experiment and comparison model. Section III considers the power distribution while Section IV considers the velocity distribution. A summary is provided in Section V.

II. EXPERIMENT AND MODEL

The goal of the Yscat94 experiment was to obtain measurements of the radar cross section under a wide variety of environmental conditions in Lake Ontario. The fetch varies from 1 to 300 km but averages about 6 km. The Yscat instrument is an ultra-wide band (2-18 GHz) Doppler radar. The antenna system provides a nearly constant 5° beam width over most of the operating bandwidth. Ten Hz measurements of the Doppler bandwidth, Doppler centroid, and echo power were made along with 30 s averages of wind speed and direction at 10 m, rain, temperature, and rms weight height [1].

A simple model is used to compare Yscat94 data with scattering theory. The small Yscat antenna footprint (1 m) is on the order of a few "coherence areas," the typical size over which the surface scatterers are correlated. In the composite model the water surface is composed of small independent "patches" whose individual cross sections are given by small perturbation theory. The patches are tilted by underlying long waves or swell which changes the cross section by changing the local incidence angle. The total cross section is the sum of the cross section of the individual patches illuminated by the antenna footprint. The distribution is thus dependent on the distribution of the wave slopes, which is, in turn, dependent on the wave spectrum. In our simple model the reflection coefficients are given by small perturbation theory [4]. The Donelan wave spectrum [3], which was developed at the same site as Yscat94, is used.

The composite model requires a cutoff between long waves (those that tilt the surface) and very short (Bragg) waves. Since the Yscat footprint size is approximately 1 m, we have computed the slope as the first order fit to a stochastic realization of a 2/3 meter-sized water surface in the simulation. The distribution of slopes is then calculated by forming a random realization of the sea surface with amplitudes from the Donelan spectrum and uniformly-distributed phases, and allowing the various spectral components to propagate through the antenna footprint according to the wave dispersion equation.

The measured velocity of the Bragg waves is affected by wind drift and hydrodynamic modulation by the underlying waves. Each of the small patches in the composite model is tilted and advected by any underlying long waves or swell which changes its cross section by changing the apparent incidence angle and line-of-sight (LOS) velocity. Wedge scatterers and breaking waves are associated with longer wavelength waves and therefore have different phase velocities.

In the simulation the LOS velocity of a point is determined by integrating the LOS velocity over the range of wave frequencies thought to contribute to the velocity of the patch. The patch velocity found by integrating the point velocities over the entire patch. The intrinsic velocity of the Bragg scatterers (both upwind and downwind components) is then added to the LOS velocity of the patch along with the drift velocity. Note that the average centroid velocity measured by a scatterometer will be the weighted average of the upwind and downwind traveling waves plus the superimposed wind drift. While this velocity model is overly simplified, it is useful for comparison to Yscat94 data.

III. POWER DISTRIBUTION

Histograms of empirical and simulated measurements were computed using 0.5 dB bins centered on the mean return power. Each histogram consists of 600 measurements, corresponding to one minute of 1/10 s measurement. Once the individual histograms have been computed, all of the histograms which correspond to the same measurement parameters (e.g. wind speed, direction, frequency) are averaged together to estimate the average histogram. Since we are interested in the average shape of the distribution, the mean of each distribution is first normalized and the corresponding bins averaged together. The mean is then added back in. This was done to minimize the effects of slow changes in system gain or other parameters which aren't relevant to the shape of the distribution. A sample result is shown in Fig. 1.

As long as the range of incidence angles is small, the dependence of the radar cross section on incidence angles is approximately exponential and the resulting distribution is log-normal [2]. The Weibull distribution has also been suggested [7]. The normalized histograms are

This work was supported by the NASA Innovative Research Program under NASA contract NAGW-2875.

0-7803-3068-4/96$5.00©1996 IEEE

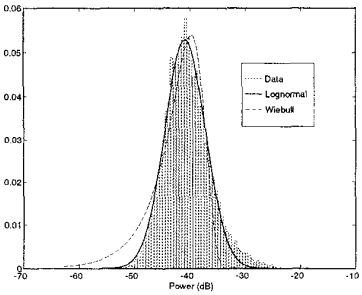

Figure 1. Sample histogram and fitted distributions.

fitted to log-normal and Weibull distributions by minimizing the L2 norm [6] as illustrated in Fig. 1. While the empirical distribution has more of an upper tail than the log-normal, a similar tail is visible in the simulation data and is thus predicted by the composite model. Since the log-normal describes the actual distributions well, the mean and variance of log-normal distribution serve as a compact and useful parameterization of the actual data distribution. In this paper we emphasize the log-variance results summarized in Fig. 2.

The log-variance decreases with increasing incidence angle. This agrees with the composite model which predicts smaller variance as the slope of the incidence angle dependence (m) decreases and the antenna footprint increases. Since the V-pol incidence angle dependence of σ^o is much less for moderate incidence angles [6] the V-pol log-variances should be less than the corresponding H-pol log-variances, a conclusion supported by the data. Note that the V-pol log variances are much less variable than the H-pol.

The log-variances do not appear to change strongly with wind speed. The simulation results have similar log-variance values and exhibit the same incidence angle dependence. However, the simulation results suggest that the log-variance should vary more with wind speed. When viewed in light of the composite model, it is clear that the fluctuations of the local incidence angle, which increase with wind speed, should increase the log-variance of the radar return as in the simulation. However, if the coherence area of the surface decreases with wind speed, the antenna footprint averages over more independent areas, decreasing the variance of the measurements. If the coherence length is decreased by a factor of two over the wind speed range (corresponding to an increase by a factor of four in the number of independent areas) the resulting wind speed dependence in the simulation is similar to that observed in the empirical data. While some empirical work has been done on the size of the coherence area the results were insufficient to determine the wind speed dependence [8]. Our results suggest that coherence area decreases with increasing wind speed.

Representative generalizations can be made by comparing simulation and empirical results. Qualitatively, the simulations compare quite well with the data for most cases. At moderate (30°-50°) incidence angles and wind speeds the distributions are quite log-normal. A distinct upper tail is visible (see Fig. 1) in both the simulation and the empirical data. It has been suggested that the upper tail is caused by additional scatterers such as wave breaking or sea-spikes. However, this cannot be the case in the simulated data since no attempt was made to include wave breaking in the model. There are smaller tails at mid-incidence angles (40° and 50°) suggesting that the source of the tails might be the "nonlinearity" of the slope dependence of σ^o, which is more severe at the extremes of the incidence angle range. Since the tails are visible in both the simulation and empirical data, care must be taken when interpreting the upper tail of the distribution as the result of non-Bragg scattering. At least a portion of this upper tail can be explained by the composite model [6]. At 20° incidence angle, the simulation data shows evidence of quasi-specular scattering as a spike in the distribution suggesting that Bragg scattering alone can not adequately describe this case. The spike is not visible in the empirical data.

At 60° incidence angle a strong lower tail develops in the simulation data due to the steep roll off of the Bragg contribution to the model that occurs at about 70° [6]. However, this tail is absent in the empirical data, suggesting that some mechanism is adding to the incidence angle dependence as the Bragg contribution drops off. It has been noted by several researchers that the mean radar cross section does not drop off with incidence angle as predicted by Bragg scattering [9]. It has also been postulated that either wave breaking or wedge scattering becomes important at high incidence angles [9]. Since breaking waves occur relatively infrequently, the distribution of a combination of wave breaking and Bragg scattering might appear very much like that of Bragg scattering alone, with a few high power events in the upper tail raising the overall mean. On the other hand, the distribution of a wedge scattering plus Bragg scattering model could appear like the Bragg only distribution with the lower tail being truncated by the addition of the low cross section wedge scattering. The lack of a lower tail in the 60° incidence angle data supports this latter description of wedge plus Bragg scattering.

IV. VELOCITY DISTRIBUTIONS

The distribution of the radar return as a function of frequency gives a measure of the range of velocities under illumination by the radar. To compute the Doppler distributions the discrete power measurements are binned according to the velocity estimated for that measurement. Histograms of the Doppler measurements for a given radar parameter set are averaged together and normalized to produce distributions. While slightly skewed, the distributions are nearly normal.

The centroid of the Doppler spectrum is a measure of the effective LOS velocity of the surface as seen by the radar. The LOS velocity predicted by the model is easily determined via the simulation and sheds some light on the qualities of the composite model. At 20° and 30° incidence the model predicts the Doppler centroid velocities quite well for both V-pol and H-pol. Both the magnitude and the measured wind drift are in good agreement between the model and the empirical data. At 40° and 50° incidence the model significantly under-predicts the Doppler centroids at low wind speeds but the difference decreases with increasing wind speed. The wind drift predicted by the model is slightly high. At 60° incidence the model significantly under-predicts the Doppler centroids for all wind speeds by about 50%. This behavior is typical of all the frequencies under consideration.

This latter case points out a significant deficiency in the simple model used here. Several assumptions have been made which affect the centroid calculation. First, the assumption made that the upwind traveling Bragg waves are 1/2 the amplitude of the downwind traveling waves is only tenuously supported by empirical data. Changing the relationship between the upwind and downwind traveling waves has a significant effect on the predicted velocity of the Bragg waves. In addition, the hydrodynamic modulation of the small wave spectrum has been completely ignored in the simple model. Hydrodynamic modulation suggests that an underlying wave "stresses" the small Bragg waves as it passes. The result is a modulation of the amplitude of the Bragg waves which is coherent with the underlying long waves. The ensuing cross section is dependent on the relative phase, φ, of the underlying dominant wave. Adding hydrodynamic modulation to the model would move the peak cross section on the phase of the underlying waves and, hence, change the measured Doppler centroid. Movement of the peak

Bragg spectral amplitude to a faster portion of the wave, might explain the discrepancy between the model and the empirical data.

We note that there is no evidence of high speed scatterers in the Doppler centroid data for incidence angles less than 60°. Although the empirical velocity measurements can be slightly higher than those predicted by the simple simulation, they are on the order of those predicted for Bragg-type scatterers rather than those of breaking waves or of scattering wedges.

The Doppler distribution emphasizes higher-power portions of the return. To study the lower-power portion, the power-velocity histograms are normalized by the total number of measurements in each bin, rather than with the total power in the whole signal. The resulting distributions are called the average cross section velocity distributions. In general, the average cross section velocity distributions are similar for the empirical and simulated data. Though there is an offset in the distribution peaks, the slope of the slow speed dependence, and the general shape of the velocity profile is in very good agreement, suggesting that the composite model of Bragg scattering is in fact valid over much of the range observed by the Yscat radar. However, at 60° incidence angle and to a lesser extent at 50°, the upwind, V-pol empirical distributions are narrower than the predicted distributions.

While the scattering mechanism is the same for both V-pol and H-pol the majority of the power is scattered from a rather narrow region of the wave velocity profile [6]. Because this region is different between V-pol and H-pol, there is some velocity difference between the polarizations. In both the empirical and simulated data the H-pol return is consistently "faster" than the corresponding V-pol return. This difference is likely due to the differences between the slope-cross section relationship, which is steeper for H-pol than V-pol [4]. In any case, the differences between the H-pol and V-pol velocities are consistent with Bragg scattering.

Our results suggest that the composite scattering model accounts for the majority of the characteristics of the velocity statistics [6]. Based on the theoretical velocity of breaking waves, contributions from these events would increase the width of the Doppler distributions. However, if these events occur very infrequently, their effects may not be visible in the average Doppler histogram.

V. SUMMARY

The simplified model used in this paper is based on the composite model. The simulation data appears to agree with the empirical data qualitatively, although the variance of the simulated data shows more wind speed dependence than is evident in the empirical data. It is suggested that a decrease in the coherence area can account for this lack of wind speed dependence in the empirical data.

The composite model accurately predicts the incidence angle dependence of the distribution variance, as well as the differences between the H-pol and the V-pol distributions. Simulations show that the model qualitatively agrees with the shape of the empirical distributions. In particular, the region from 30° to 50° incidence angle seems to be in good agreement with the composite model, with no evidence of additional scattering mechanisms in the empirical data. The simulation also reveals that the upper tail of the observed distribution can be explained within the composite model. Quasi-specular scattering seems to be very important at 20° and wave breaking contributions are evident at 60°.

At 20° - 40° incidence angles, the simulation accurately predicts the observed Doppler centroids. At 50° and 60° the simulation under-predicts the Doppler centroids. This may be due to the hydrodynamic modulation transfer function. The composite model predicts a slight difference in the Doppler centroids of the H-pol and V-pol

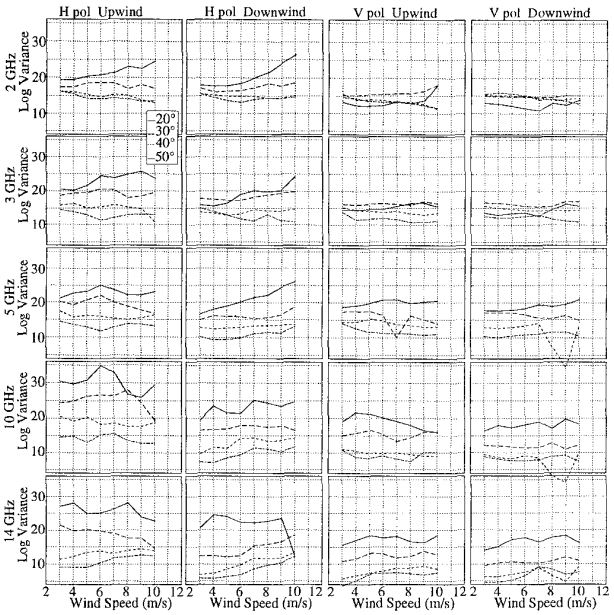

Figure 2. Log variance vs. wind speed.

data, a difference found in the empirical data. No evidence for a significant contribution from fast scatterers is found for incidence angles less than 60°.

REFERENCES

[1] D.G. Long, R.S. Collyer, R. Reed, and D.V. Arnold, "Dependence of the Normalized Radar Cross Section of Water Waves on Bragg Wavelength–Wind Speed Sensitivity," to appear, *IEEE Trans. Geosc. Rem. Sens.*, 1996.

[2] B.L. Gotwols and D.R. Thompson, Ocean microwave backscatter distributions, *J. Geophys. Res.*, vol. c5, no. 99, pp. 9741–9750, 1994.

[3] M.A. Donelan, J. Hamilton, and W.H. Hui, Directional spectra of wind-generated waves, *Phil. Trans. Royal Soc. London*, vol. 315, no. A, pp. 509–562, 1985.

[4] W.J. Plant, A two scale model of short wind-generated waves and scatterometery, *IEEE Trans. Geosc. Rem. Sens.*, vol. 91, no. 9, pp. 10735–10749, 1986.

[5] M.A. Donelan and W.J. Pierson, Radar scattering and equilibrium ranges in wind generated waves with application to scatterometry, *IEEE Trans. Geosc. Rem. Sens.*, vol. 92, no. C5, pp. 4971–5029, 1987.

[6] R. Reed, "Statistical Properties of the Sea Scattered Radar Return," Ph.D. Dissertation, Brigham Young University, Provo, UT, 1996.

[7] D.B. Trizna, Statistics of low grazing angle radar sea scatter for moderate and fully developed ocean waves, *IEEE Trans. Ant. Prop.*, vol. 39, no. 12, pp. 1681–1690, 1991.

[8] W.J. Plant, E.A. Terray, and R.A. Petit, The dependance of microwave backscatter from the sea on illuminated area: Correlation times and lengths, *J. Geophys. Res.*, vol. 99, no. C5, pp. 9705–9723, 1994.

[9] D.R. Lyzenga, A.L. Maffet, and R.A. Schuman, The contribution of wedge scattering to the radar cross section of the ocean surface, *IEEE Trans. Geosc. Rem. Sens.*, vol. GE-21, no. 4, pp. 502–505, 1983.